PS Visualization and Quantification of Deeply Buried Paleokarst Reservoirs in Tahe Oilfield, Tarim Basin, China*

Fei Tian[1], Qiang Jin[1], Yang Li[2], Hong-fang Zhang[2], and Xun Kang[1]

Search and Discovery Article #20257 (2014)**
Posted July 24, 2014

*Adapted from poster presentation given at 2014 AAPG Annual Convention and Exhibition, Houston, Texas, April 6-9, 2014

[1]School of Geosciences, China University of Petroleum, Qing Dao, China (upc_tianfei@126.com)
[2]China Petroleum and Chemical Corporation, Sinopec, Beijing, China

Abstract

Mapping and quantify 3-D construction of the paleokarst reservoirs is a challenge in deeply buried (>5500m) heterogeneous carbonate system, as their irregular geometry and complex filling materials. Well-logging constrained acoustic impedance seismic dataset and seismic attribute analysis combined with 3-D visualization technology provide a significant amount of visible information about paleokarst reservoirs' features in Tahe oilfield, Tarim basin. This paper describes an integrated approach to visualize and quantify the paleokarst reservoirs. First, caves' recognize equation is developed using conventional well-logging data, which is demarcated from core and image logs with a cave resolution of approximately 0.5 m. Second, time-depth conversions for 97 wells are identified one by one, and the recognition results in the signal wells are tied to seismic dataset. Third, after determining the cutoff values of the host rocks and the caves in acoustic impedance, the impedance inversion volume can recognize the spatial construction of the paleokarst reservoirs effectively. Forth, the 3-D mapping and visualization of the paleokarst reservoirs are achieved by tracing the distribution of caves. Fifth, based on the 3-D 'geobody' and karst genetic theory, comparing with spatial geometry of the Mammoth Cave, the Tahe paleokarst reservoirs are divided into epikarst, vadose and runoff zones. Additionally, the genetic types of them are identified, i.e. chamber caves, main channel, branch channel etc. Using 3-D visualized geobody, the length, width, area, volume of different genetic types are calculated, and the chamber caves and main channels are pointed out as prior targets for hydrocarbon exploration. Using 3-D visualization technology, the spatial construction of paleokarst reservoirs is delineated; combined with the karst hydrodynamics theory, vertical zones and genetic types of the reservoir are divided; the entrances, exits, collapses and relative high points of the cave

systems are identified; the quantification of each genetic type is calculated from line, area to volume. All achievements above provide detailed information of the reservoir for structural model, geological model, hydrocarbon exploration and can be applied to other similar paleokarst oilfields.

Visualization and Quantification of Deeply Buried Paleokarst Reservoirs in Tahe Oilfield, Tarim basin, China

Fei Tian[1], Qiang Jin[1], Yang Li[2], Hong-fang Zhang[2], Xun Kang[1]

[1]China University of Petroleum, School of Geosciences,Qingdao,266555, China;

[2]China Petroleum and Chemical Corporation, Beijing 100728, China E-mail: upc_tianfei@126.com

Paleokarst

- Developing near the surface of unconformity
- World-class hydrocarbon reservoirs
- Irregular geometry and complex filling materials
- Four zones:epikarst ,vadose,runoff, phreatic

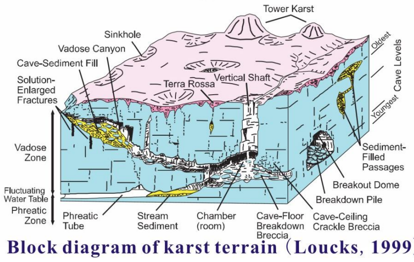

Block diagram of karst terrain（Loucks, 1999）

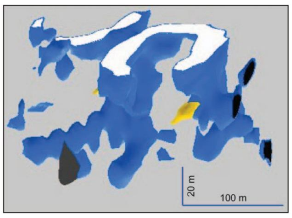

Visualization of paleocave（Zeng, 2011）

Paleokarst Oilfields in China

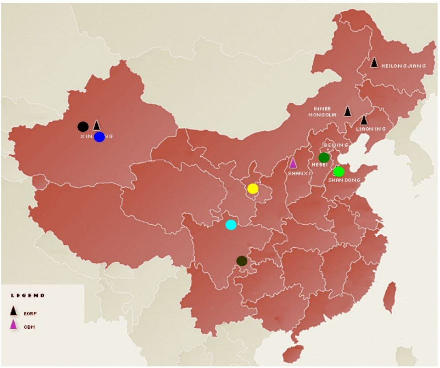

- Naxi Gasfield
- Weiyuan Gasfield
- Renqiu Oilfield
- Shengli Oilfield
- Changqing Oilfield
- Tarim Oilfield
- Tahe Oilfield

Geological background of Tahe Oilfield

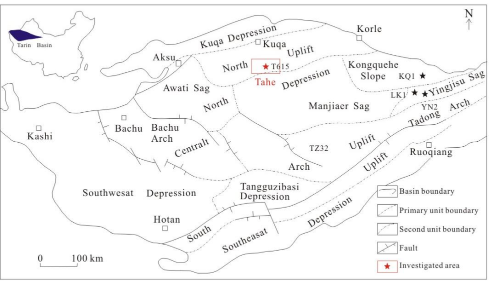

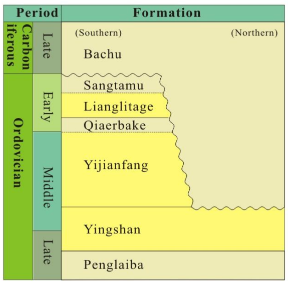

- In northern Tarim Basin, Northwest China
- Three main kast reservoir formations: Lianglitage, Yijianfang, Yingshan

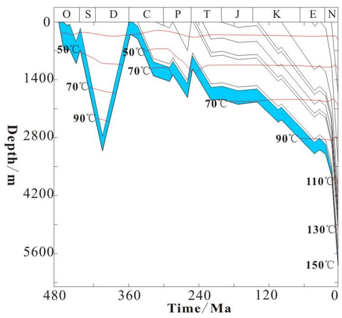

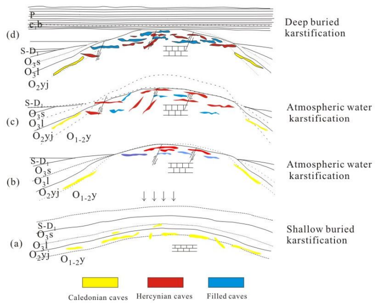

Burial history of well S75 Karstification of Tahe Oilfield

- Middle Caledonian: Shallow buried karstification
- Early Hercynian: Atmospheric water karstification
- After Hercynian: Deep buried karstification

Characters of Fracture-Caves

Outcrop observation

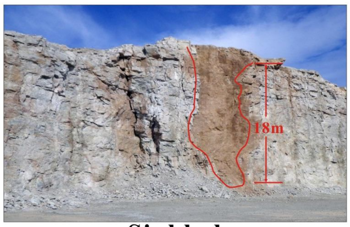

Sinkhole

Main channel

Branch channel

Tip channel

Multi-layers caves

Multi-layers caves

- Fractures developed around caves
- Multi-types of fills in the cave
- There are many cave players
- Results of multi-stages karstification

Cave fills in core

Clastic sediment

Breccias

Chemical fills

Fracture-cave combination

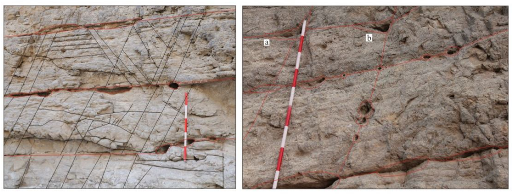

In outcrop

In core

Fractures in core

High angle

Medium angle

Low angle

High density

Low density

Conventional Recognize Methods

Abnormal Drilling

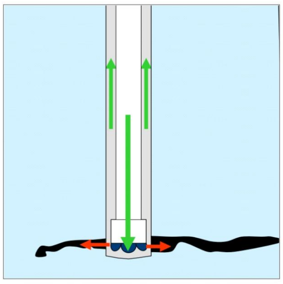

3-D Seismic Reflection

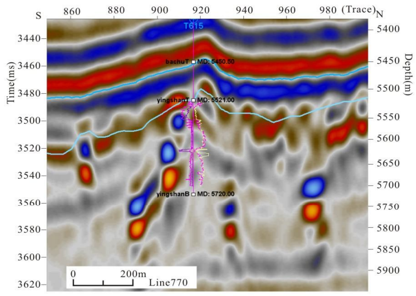

Image logging

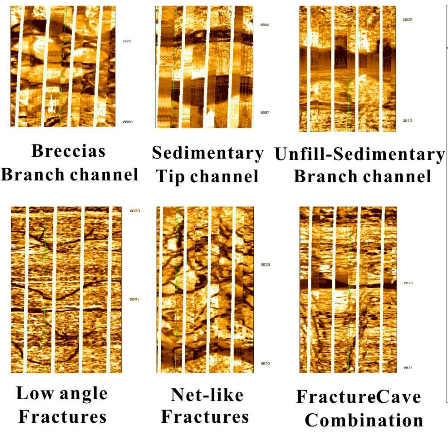

Conventional Logging

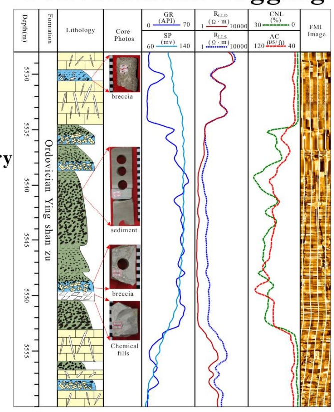

New parameters

Shale Content

$$SH_1=\frac{GR-GR_{\min}}{GR_{\max}-GR_{\min}} \qquad V_{sh}=\frac{2^{2\times SH_1}-1}{3}$$

Absolute of DLL

$$K_3=\left|\frac{1}{R_{LLS}}-\frac{1}{R_{LLD}}\right|$$

Cave Recognition

Multi-parameters standard-weighted method

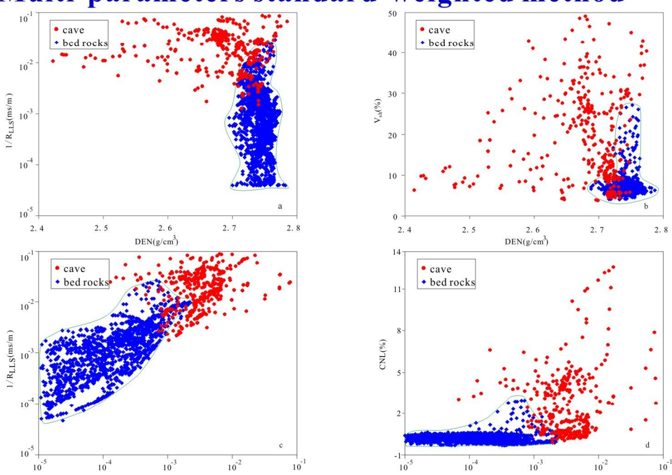

Five parameters cros-plot to recognize cave

	$1/R_{LLS}$-DEN	V_{sh}-DEN	$1/R_{LLS}$-K_3	CNL-K_3
Bed rock	$1/R_{LLS}<0.05$ DEN>2.63	$V_{sh}>25\%$ DEN>2.63	$1/R_{LLS}<0.05$ $K_3<0.003$	CNL<2% $K_3<0.003$
Cave	$1/R_{LLS}>0.005$ DEN<2.75	$V_{sh}>10\%$ DEN<2.75	$1/R_{LLS}>0.005$ $K_3>0.002$	CNL>0% $K_3>0.002$

$$P=0.4\times X_1+0.19\times(X_2-X_3)+0.25\times X_4+0.16\times X_5$$

$$P=\sum_{i=1}^{n}C_i\times X_i \qquad \sum_{i=1}^{n}C_i=1$$

P>0.3is cave section

X_i is normalized parameters
X_1: normalized K_3
X_2: normalized CNL
X_3: normalized DEN
X_4: normalized $1/R_{LLS}$
X_5: normalized V_{sh}

Cave Fills Recognition

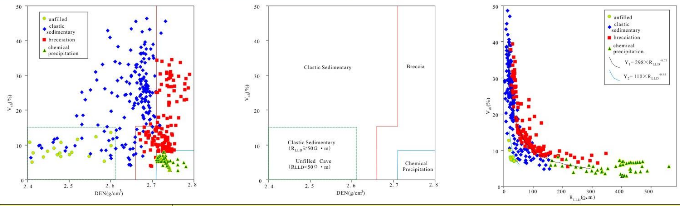

Fill types	Dividing Section
Unfillsection	DEN<2.61, $R_{LLD}\leq 50$, $V_{sh}<15\%$
Sedimentary	①DEN<2.61, $R_{LLD}\leq 50$, $V_{sh}\geq 15\%$; ②DEN<2.61, $R_{LLD}\geq 50$
	③2.61≤DEN<2.68 ④2.68≤DEN<2.71, $V_{sh}\geq 15\%$
Breccia	①2.68≤DEN<2.71, $V_{sh}<15\%$; ②2.71≤DEN, $V_{sh}\geq 8\%$
Chemical Fills	2.71≤DEN, $V_{sh}<8\%$

Fractures Recognition

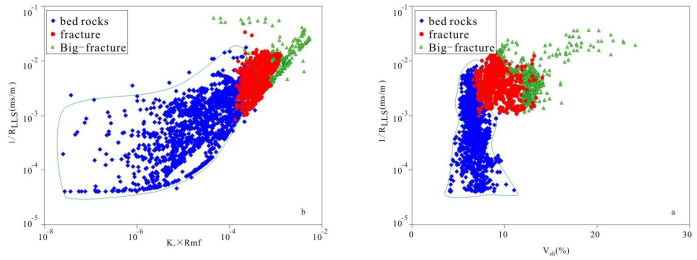

$$M=0.21\times Y_1+0.43\times Y_2+0.36\times Y_3$$

Y_1: normalized V_{sh}
Y_2: normalized $1/R_{LLS}$
Y_3: normalized K_3*Rmf

M>0.45 is fracture-cave combination
0.16<M<0.45 is fracture

Fracture Angle

$$Y=\frac{R_{LLD}-R_{LLS}}{\sqrt{R_{LLD}\times R_{LLS}}}$$

Fracture Porosity

$$\varphi_{fr}=\left(\frac{A_1}{R_{LLS}}+\frac{A_2}{R_{LLD}}+A_3\right)\times R_{mf}$$

Angle	Y	A_1	A_2	A_3
Low	Y<0	-0.992417	1.97247	0.00031829
Medium	0.1≤Y≤0	-17.6332	20.36451	0.00093177
High	Y>0	8.522532	-8.242788	0.00071236

Recognition Results of Core and FMI Section

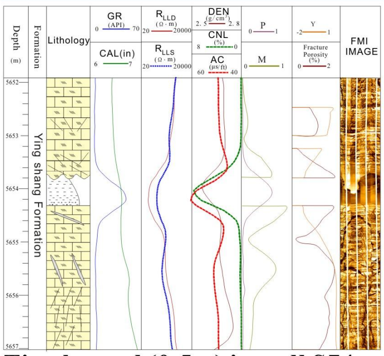

Tip channel (0.5m) in well S74

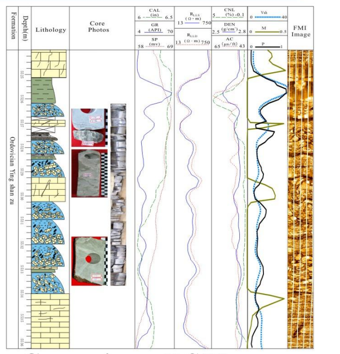

Caves in well S75

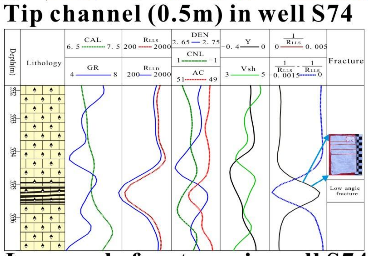

Low angle fractures in well S74

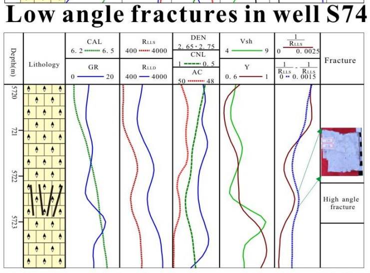

High angle fractures in well S75

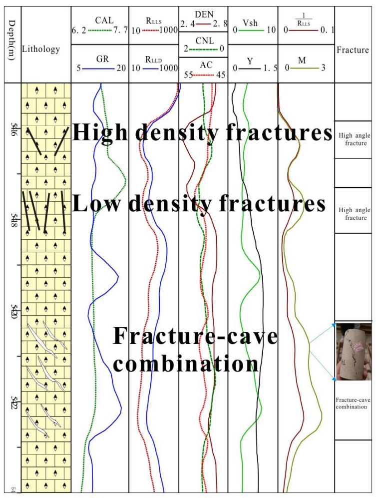

Recognition Results of Fracture-cave

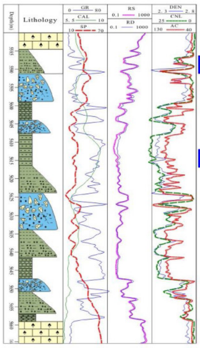

- Fractures
  Low angle
  High density
- Fills
  Sedimentary
  7 cycles
  + Breccias
  4 cycles

Chamber cave(74m)
in Well TK409

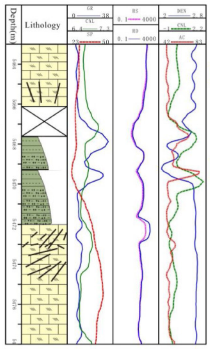

- Fractures
  High angle
  High density
- Fills
  Sedimentary
  2 cycles
  +Unfilled cave

Main channel(6m)
in Well TK411

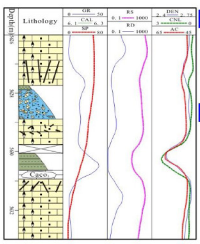

- Fractures
  High angle
  Low density
- Fills
  Unfilled cave
  Sedimentary
  Breccias
  Chemical fills

Branch channel(1-1.3m)
in Well TK633

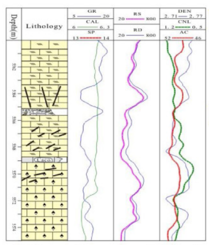

- Fractures
  High angle
  High density
- Fills
  Breccias
  Chemical fills

Tip channel (0.3m)
in Well TK421

Table 1 Caves recognition results in seismic data

Well	NO. in depth	Cave Top	Cave Bottom	Cave Height	Distance to T74	Conventional volume	Impedance volume	FMI
T615	A2	5534.1	5554.6	20.5	13.1	√	√	√
T615	A10	5631.3	5639.9	8.6	110.3	×	√	√
T615	A11	5669.6	5675.9	6.3	148.6	×	×	√
T615	A9	5624.6	5627.8	3.2	103.6	×	√	√
T615	A3	5555.5	5558.3	2.8	34.5	×	√	√
T615	A12	5677.4	5679.4	2.0	156.4	×	×	√
T615	A4	5561.6	5563.5	1.9	40.6	×	×	√
T615	A6	5567.6	5569.3	1.7	46.6	×	×	√
T615	A8	5572.5	5574.1	1.6	51.5	×	×	√
T615	A13	5685.0	5686.4	1.4	164.0	×	×	√
T615	A1	5529.4	5530.6	1.2	8.4	×	≈	√
T615	A5	5566.4	5567.0	0.6	45.4	×	×	√
T615	A7	5570.5	5570.9	0.4	49.5	×	×	√
TK730	B8	5563.1	5581.3	18.2	44.1	√	√	
TK730	B10	5603.4	5611.3	7.9	84.4	√	√	
TK730	B7	5558.3	5561.4	3.1	39.3	×	√	
TK730	B9	5588.9	5591.3	2.4	69.9	×	√	
TK730	B6	5556.0	5557.1	1.1	37.0	×	≈	no data
TK730	B2	5528.9	5529.8	0.9	9.9	×	too small and too close to divided respectively	
TK730	B4	5540.9	5541.6	0.7	21.9	×		
TK730	B3	5530.8	5531.4	0.6	11.8	×		
TK730	B5	5543.8	5544.4	0.6	24.8	×		
TK730	B1	5525.8	5526.1	0.3	6.8	×		

√: recognized, ×: unrecognized, ≈: uncertain

Time-Depth Calibration

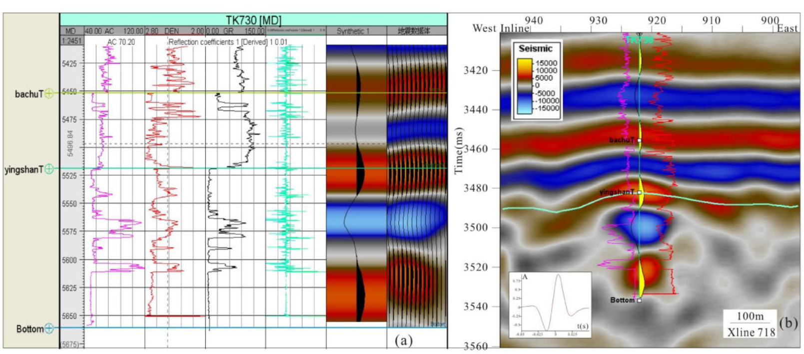

Optimization of Seismic Data

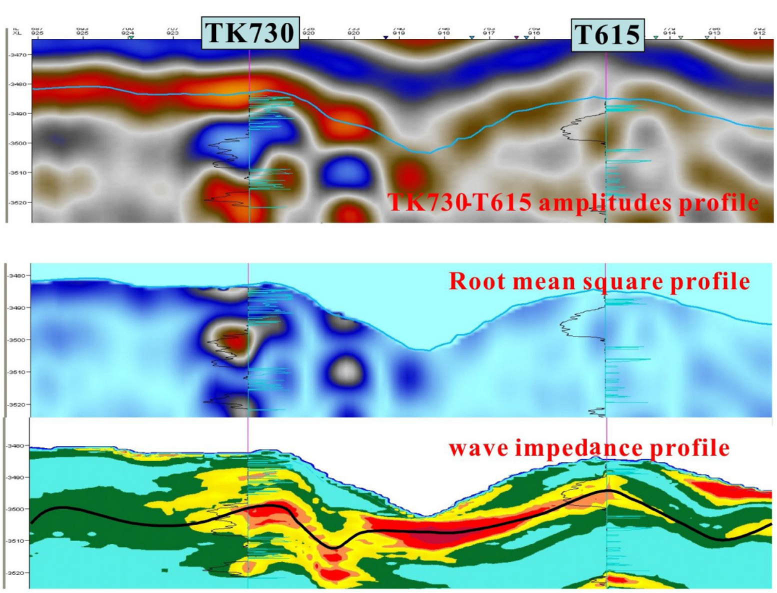

- Comparison of different attribute seismic profiles
- Wave impedance inversion reflects caves better
- The larger and more continuous caves were chosen
  We trace their center to interpret the karst construction

Applied in the Area of Well T615

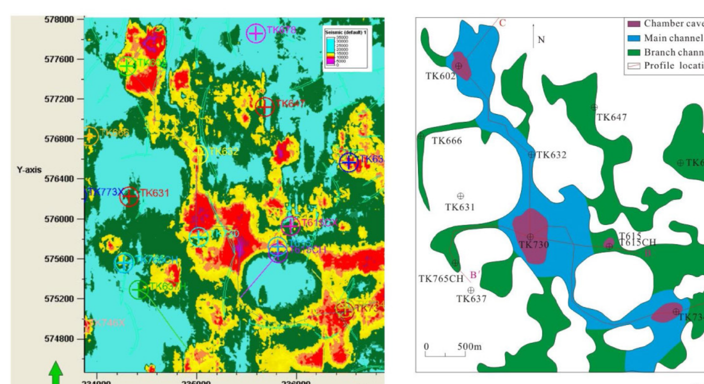

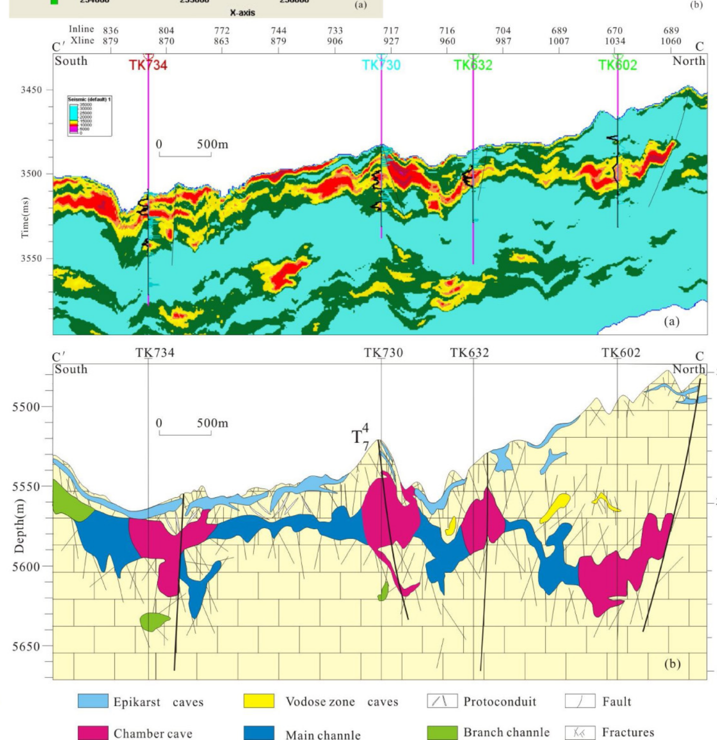

Visualization and Quantification

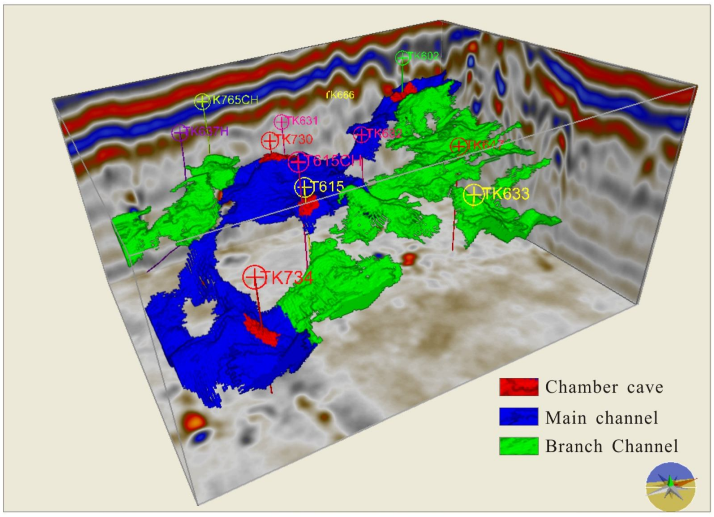

Table 2 Statistics of paleokarst reservoirs of Well T615 area in run-off zone 1

Cave Type	Number	Length (m)	Width (m)	Area (m²)	Area Ratio	Volume (m³)	Volume Ratio
Chamber caves	4	80610	40-330	421425	10.88%	20367000	18.57%
Main channel	1	7080	130-720	1776600	45.86%	57574000	52.49%
Branch channel	8	2901800	30-420	1675575	43.26%	31741000	28.94%

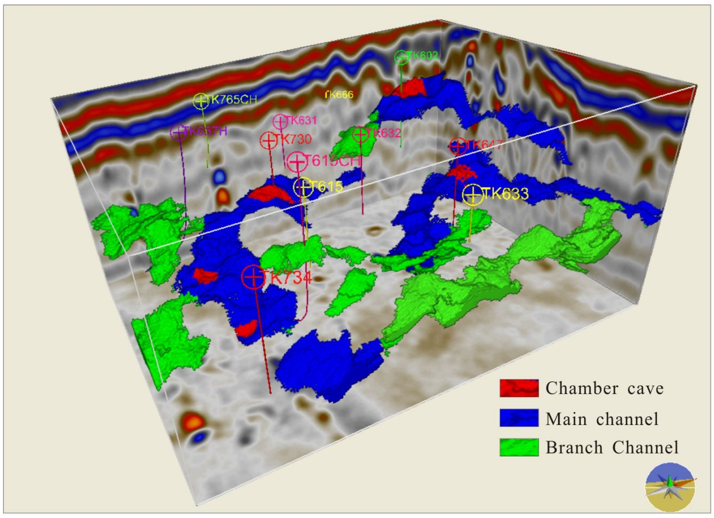

Table 3 Statistics of paleokarst reservoirs of Well T615 area in run-off zone 2

Cave Type	Number	Length (m)	Width (m)	Area (m²)	Area Ratio	Volume (m³)	Volume Ratio
Chamber Cave	5	60-240	90-260	235575	4.72%	9017000	6.81%
Main channel	3	1400-2200	130-500	2710800	54.27%	76587000	57.85%
Branch channel	5	400-1500	60-230	2048850	41.02%	46793000	35.34%

Geological Model

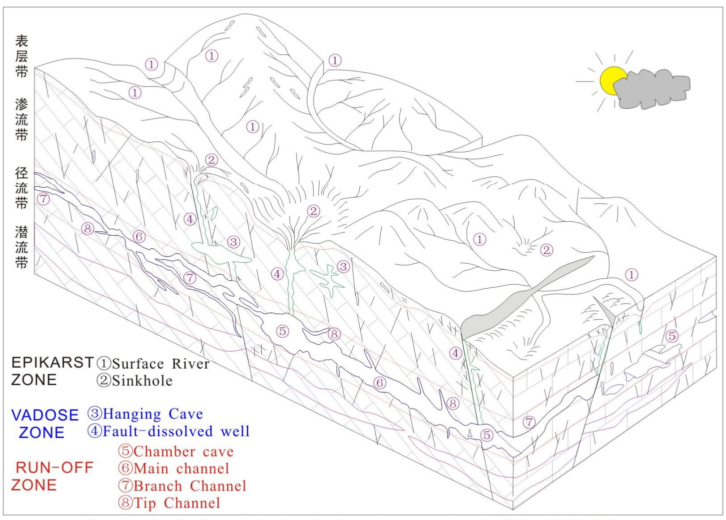

The geological model of paleokarst reservoirs in Tahe Oilfield

Discussion and Conclusion

- Demarcated from core and image logging information, we optimize DEN, CNL, Vsh, CLLS and ΔC and build a cave recognition equation, of which the coincidence of small cave (H <1 m) is greater than 81%; next, we optimize CLLS, Vsh and ΔC×Rmf and build a fracture and protoconduit recognition equation, the coincidences of which are greater than 82%.

- After detailed time-depth conversions for each of the 97 wells in Ordovician strata, the interpretation results of single wells are demarcated on the acoustic impedance inversion volume. In certain wells, which are demarcated by well-logging, the resolution of the volume is approximately 3 m, and the descriptions of the paleokarst between wells are also reliable.

- This method is applied in the area of Well T615, and the construction of paleokarst in this area is interpreted. The run-off zone has developed 2 layers of caves. The length, width, area, volume of different genetic types are calculated, and the chamber caves and main channels are pointed out as prior targets for hydrocarbon exploration.

- The major contribution of this integrated method of combining cores, well logs and acoustic impedance inversion volume is to detect precisely and analyze the construction of paleokarst reservoirs in three-dimensional space.

Analyzing the genetic relationships and control factors of the geological concept model including epikarst zone, the vadose zone and the run-off zone is the next study objective.

Our study provides a reliable and precise description of the construction of deeply buried paleokarst reservoirs and maybe applied to similar subsurface paleokarst systems in other areas.

Acknowledgements

Special thanks to China national basically research program-2011CB201001, Tahe Oilfield Sinopec for providing data. We also thank numerous colleagues.

References

Loucks. R. G., 1999. Paleocave carbonate reservoirs: origins, burial-depth modifications, spatial complexity and reservoir implications. AAPG 83(11):1795~1834

Zeng Hongliu, Wang G, Janson X, Loucks R, Xia Y. Characterizing seismic bright spots in deeply buried, Ordovician Paleokarst strata, Central Tabei uplift, Tarim Basin. Geophysics,2011, 76(4): B127~B137